Predicting Solvent Stability in Aprotic Electrolyte Li–Air Batteries: Nucleophilic Substitution by the Superoxide Anion Radical ($O_2^{\bullet-}$)

ARTICLE *in* THE JOURNAL OF PHYSICAL CHEMISTRY A · SEPTEMBER 2011

Impact Factor: 2.69 · DOI: 10.1021/jp2073914 · Source: PubMed

9 AUTHORS, INCLUDING:

Vincent Giordani
Liox Power, Inc.
23 PUBLICATIONS **614** CITATIONS
SEE PROFILE

Mario Blanco
King Abdullah University of Science and Tec…
64 PUBLICATIONS **1,705** CITATIONS
SEE PROFILE

Jasim Uddin
California Institute of Technology
44 PUBLICATIONS **1,521** CITATIONS
SEE PROFILE

Dan Addison
Independent Researcher
21 PUBLICATIONS **301** CITATIONS
SEE PROFILE

THE JOURNAL OF PHYSICAL CHEMISTRY A

ARTICLE

pubs.acs.org/JPCA

Predicting Solvent Stability in Aprotic Electrolyte Li−Air Batteries: Nucleophilic Substitution by the Superoxide Anion Radical ($O_2^{\bullet-}$)

Vyacheslav S. Bryantsev,* Vincent Giordani, Wesley Walker, Mario Blanco,† Strahinja Zecevic, Kenji Sasaki, Jasim Uddin, Dan Addison, and Gregory V. Chase

Liox Power, Inc., 129 North Hill Avenue, Suite 103, Pasadena, California 91106, United States

Supporting Information

ABSTRACT: There is increasing evidence that cyclic and linear carbonates, commonly used solvents in Li ion battery electrolytes, are unstable in the presence of superoxide and thus are not suitable for use in rechargeable Li−air batteries employing aprotic electrolytes. A detailed understanding of related decomposition mechanisms provides an important basis for the selection and design of stable electrolyte materials. In this article, we use density functional theory calculations with a Poisson−Boltzmann continuum solvent model to investigate the reactivity of several classes of aprotic solvents in nucleophilic substitution reactions with superoxide. We find that nucleophilic attack by $O_2^{\bullet-}$ at the *O*-alkyl carbon is a common mechanism of decomposition of organic carbonates, sulfonates, aliphatic carboxylic esters, lactones, phosphinates, phosphonates, phosphates, and sulfones. In contrast, nucleophilic reactions of $O_2^{\bullet-}$ with phenol esters of carboxylic acids and *O*-alkyl fluorinated aliphatic lactones proceed via attack at the carbonyl carbon. Chemical functionalities stable against nucleophilic substitution by superoxide include *N*-alkyl substituted amides, lactams, nitriles, and ethers. The results establish that solvent reactivity is strongly related to the basicity of the organic anion displaced in the reaction with superoxide. Theoretical calculations are complemented by cyclic voltammetry to study the electrochemical reversibility of the $O_2/O_2^{\bullet-}$ couple containing tetrabutylammonium salt and GCMS measurements to monitor solvent stability in the presence of $KO_2^{\bullet}$ and a Li salt. These experimental methods provide efficient means for qualitatively screening solvent stability in Li−air batteries. A clear correlation between the computational and experimental results is established. The combination of theoretical and experimental techniques provides a powerful means for identifying and designing stable solvents for rechargeable Li−air batteries.

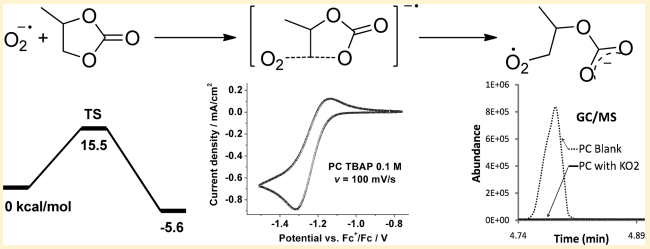

INTRODUCTION

The aprotic electrolyte rechargeable lithium−air (oxygen) battery offers one of the highest theoretical specific energies among electrochemical energy storage devices.[1−10] However, formidable scientific and technical challenges must be overcome before this promising technology becomes a viable alternative to conventional Li ion batteries. Recent developments and challenges facing Li−air batteries are summarized in several excellent reviews.[11−13] One prerequisite for the development of rechargeable Li−air batteries that have both high capacity and high cycle number is the identification of electrolyte materials that are not significantly consumed or decomposed in the air cathode during cell operation.

Recent studies at the University of St. Andrews,[14,15] Toyota,[16−18] IBM,[11,19] PNNL,[20] and ORNL[21] have shown that organic carbonate solvents, commonly used electrolytes in Li ion batteries, are unstable against oxygen reduction products formed in the air cathode of Li−air batteries. Much of the evidence comes from Fourier transform infrared (FT-IR) and Raman spectroscopy data[14−20] indicating that the primary discharge product in carbonate-based electrolytes is not lithium peroxide, Li_2O_2, but various carbonate species, such as RO—(C═O)—OLi and Li_2CO_3. Furthermore, in situ differential electrochemical mass spectrometry (DEMS) experiments[14−19] combined with ^{18}O isotopic labeling[19] reveal that, during charging of the discharged battery, CO_2 is evolved as a predominant oxidation product, most probably from the oxidative decomposition (during recharge) of lithium carbonates and alkyl carbonates. Decomposition of the solvent during cycling eventually leads to cell failure. While this failure mode may be delayed by including excess solvent to account for decomposition,[16] the costs in volume and mass of such excess solvent may be too high for practical applications.

The superoxide anion radical ($O_2^{\bullet-}$) is thought to be responsible for the decomposition of carbonate solvents.[14−20] Important evidence comes from the irreversibility of the $O_2/O_2^{\bullet-}$ redox couple in the propylene carbonate (PC) solvent containing large organic cations.[14,18,22] However, until recently, there was a lack of clear understanding of the major mechanism of decomposition of carbonate solvents by superoxide. In a recent

Received: August 2, 2011
Revised: September 29, 2011
Published: September 30, 2011

Scheme 1. Mechanism of Superoxide-Induced Decomposition of Propylene Carbonate

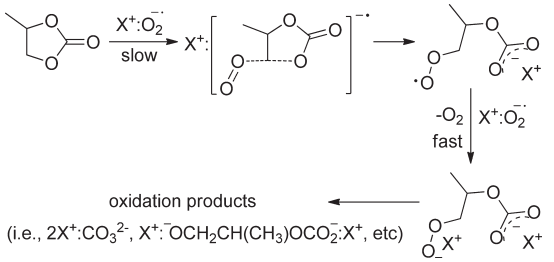

communication,[23] we use density functional theory and coupled-cluster calculations to show that the nucleophilic attack by $O_2^{\bullet-}$ at etheral carbon atoms is a common mechanism of degradation of organic carbonate solvents (Scheme 1). In the Li−air battery, lithium superoxide ($LiO_2^{\bullet}$) is a primary intermediate,[24−26] which could be either converted to Li_2O_2 (both chemically and electrochemically) or involved in the decomposition of electrolyte. The presence of Li^+ ions is expected to cause some increase in the activation energy for nucleophilic attack, because neutral $LiO_2^{\bullet}$ is less nucleophilic than the negatively charged $O_2^{\bullet-}$ ion. Indeed, by explicit inclusion of several solvent molecules, $LiO_2^{\bullet}$ was predicted[23] to be less reactive than $O_2^{\bullet-}$ in nucleophilic addition to ethylene carbonate (EC). However, the calculated activation energy (ΔG_{act} = 20.2 kcal/mol) was not sufficiently high to completely suppress the decomposition of EC.

Understanding the relationship between solvent structure and chemical stability against superoxide is critical for the selection and design of new stable electrolytes that withstand the specific chemical environment in Li−air batteries. Extensive research on the organic chemistry of $O_2^{\bullet-}$ in aprotic media has established that this anion radical may react with organic substrates via nucleophilic attack, proton/hydrogen abstraction, and/or electron transfer.[27,28] For electrolyte solvents with a relatively wide electrochemical stability window, the direct electron transfer from/to superoxide is not generally expected.[29] Solvent decomposition by superoxide through a proton abstraction mechanism will be important for weakly acidic substrates.[30−33] Calculations of acidity constants of organic solvents are underway in our laboratory to address this possibility and will be reported in a forthcoming publication. While the mechanism of proton-induced disproportionation of superoxide in aprotic solvents has been thoroughly analyzed,[30−33] the ability of superoxide to act as a strong nucleophile is much less understood.[28,34−38] For example, there have been conflicting results concerning the reaction mechanism of alkyl ester cleavage by superoxide in solution and the gas phase. It is generally believed that that liquid-phase reactions of $O_2^{\bullet-}$ with aliphatic esters occur via attack at the carbonyl carbon.[28,34−36] However, a different mechanism has been supported by mass spectrometric studies,[37,38] suggesting that $O_2^{\bullet-}$ reacts with alkyl esters in the gas phase by an S_N2 displacement process at the *O*-alkyl carbon. Hence, further investigations are required to clarify the main reaction pathways for superoxide-induced decomposition of esters and related compounds.

Herein we report the computed free energy barriers (ΔG_{act}) and reaction free energies (ΔG_r) for nucleophilic substitution of a series of aprotic solvents by the superoxide anion. These data provide a convenient means of screening for suitable solvents in Li−air batteries from first-principles calculations. The stability of a number of commercial aprotic solvents toward superoxide is also examined by studying the electrochemical reversibility of the oxygen reduction reaction[17,18,22,39−42] at a glassy carbon electrode in solutions containing 0.1 M tetrabutylammonium perchlorate (TBAP) or tetrabutylammonium bis(trifluoromethane)-sulfonimide (TBATFSI) as the supporting electrolyte. Finally, we exposed the candidate solvents to an excess amount of $KO_2^{\bullet}$ (with and without 18-crown-6 ether)[17] in acetonitrile solution and analyzed the stability of solvent chromatographic peaks from the GCMS spectra. Excellent agreement is obtained among all the chemical, electrochemical, and quantum chemical techniques in evaluating solvent reactivity with superoxide. The results clearly establish that solvent reactivity is strongly related to the thermodynamic stability of the organic anion formed during the reaction with superoxide, providing important guidelines for the selection and design of suitable electrolyte systems for Li−air batteries.

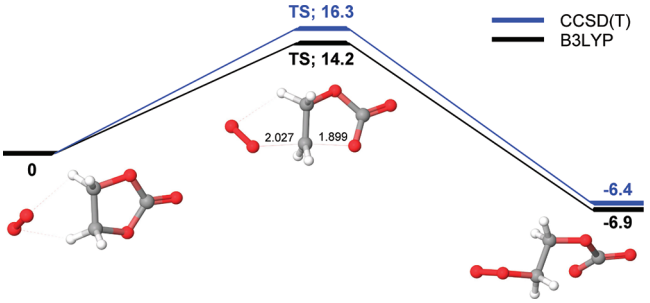

Figure 1. Comparison of reaction free energy profiles (T = 298.15 K) for superoxide addition to the etheral carbon atom of ethylene carbonate calculated at the B3LYP/aug-cc-pVTZ and CCSD(T)/aug-cc-pV5Z levels (kcal/mol). Solvent effects are included within the continuum dielectric approximation. B3LYP optimized C−O bond lengths in the transition state are shown.

METHODS

Theoretical Calculations. Electronic structure calculations were carried out using the Jaguar 7.5[43] and the NWChem 5.1[44] programs. Geometries were optimized using the B3LYP/6-311++G** method,[45,46] except for molecular complexes with explicit solvent molecules, for which the B3LYP/6-31G** method was used. In addition, single point-energy calculations were performed using the augmented correlation consistent valence polarized triple-ζ basis set (aug-cc-pVTZ),[47,48] which in general provides better overall performance for predicting reaction energetics of negatively charged ions.[23,49] As a benchmark for determining the accuracy of the B3LYP method, we employed calculations at the second-order Møller−Plesset perturbation theory (MP2)[44,50] in the aug-cc-pV5Z basis set with coupled-cluster theory[44,51−53] corrections at the CCSD(T)/aug-cc-pVDZ level. MP2 and CCSD(T) calculations used unrestricted reference wave functions, keeping core electrons frozen. Comparative calculations for superoxide addition to the *O*-alkyl carbon of ethylene carbonate showed that the use of the B3LYP/aug-cc-pVTZ method does not lead to significant differences in activation (∼2.1 kcal/mol) and reaction (∼0.6 kcal/mol) energies when compared to benchmark calculations at the extrapolated CCSD(T)/aug-cc-pV5Z level (Figure 1). The good agreement found

Table 1. Comparison of Free Energy Barriers (ΔG_{act}) and Reaction Free Energies (ΔG_r) for Nucleophilic Attack by the Superoxide Ion on Etheral Carbon Atoms of Propylene Carbonate (PC) and Ethylene Carbonate (EC) Calculated Using a Dielectric Continuum Solvent Model and a Mixed Cluster/Continuum Representation of the Solvent (kcal/mol)

	dielectric continuum model		mixed cluster/continuum model[a]	
solvent	ΔG_{act}	ΔG_r	ΔG_{act}	ΔG_r
PC	15.47	−5.64	15.12	−1.45
EC	14.22	−6.94	12.83	−6.58

[a] Four additional solvent molecules were placed in the vicinity of the reaction center. The structural model of the reaction site for EC is exemplified in Figure 2.

here thus justifies the use of the B3LYP/aug-cc-pVTZ method to probe the reactivity of aprotic solvents with superoxide.

Transition-state search was performed using a standard quasi-Newton method in Jaguar,[43] starting from the partially optimized geometry along the chosen reaction coordinate and the precalculated Hessian. The nature of all transition states obtained at the B3LYP/6-311++G** level was confirmed by the presence of a single imaginary frequency in the vibrational spectrum, corresponding to the motion along the reaction coordinate. The standard Gibbs free energy of each species in the gas phase (T = 298 K, P = 1 atm) was calculated using the rigid rotor harmonic oscillator approximation. The presence of several low frequency modes (<20 cm^{-1}) in the vibrational spectra of complexes with explicit solvent molecules would have an adverse effect on the accuracy of the vibrational entropy contributions to the reaction free energy and barrier. Therefore, these were not calculated, but were taken from the analogous reaction with no additional solvent molecules present (Table 1).

Solvation calculations were carried out using the Poisson−Boltzmann continuum model in Jaguar,[41] with the default values of solute atomic radii. The dielectric constants for propylene carbonate (PC), ethylene carbonate (EC), dimethyl carbonates (DMC), γ-butyrolactone (GBL), *N*-methyl-2-pyrrolidone (NMP), ethyl methyl sulfone (EMS), sulfolane (SFL), acetonitrile (MeCN), benzonitrile (BN), and dimethoxyethane (DME) are given in Table 2, and probe radii are defined from their molecular weights and liquid densities at room temperature as follows: 2.566 (PC), 2.354 (EC), 2.556 (DMC), 2.473 (GBL), 2.674 (NMP), 2.455 (EMS), 2.664 (SFL), 2.180 (MeCN), 2.734 (BN), and 2.749 (DME).

In modeling solvation effects, an important question arises as to whether computational results are sensitive to the presence of explicit solvent molecules surrounding the reaction system. Figure 2 provides an illustrative example of such a mixed cluster/continuum model, where four additional EC molecules were placed into the system to effectively solvate the charged species involved in the nucleophilic displacement at the etheral carbon atom of EC. A similar structural model was previously constructed for the reaction of PC with superoxide.[23] Comparison of reaction barriers and energies given in Figure 2 and Table 1 indicates that a simple dielectric continuum description of the solvent yields results that are quantitatively compatible (typically within 4 kcal/mol) with those obtained by explicitly including additional solvent molecules.

General. All solvents were purchased from Sigma-Aldrich except for dimethoxyethane and propylene carbonate, which were obtained from Novolyte. Benzonitrile, acetonitrile, ethylene carbonate, dimethoxyethane, and propylene carbonate were either battery grade or anhydrous and were used as received. γ-Valerolactone and sulfolane were dried over molecular sieves for 24 h prior to use. Finally, dimethyl methylphosphonate, triglyme, and *N*-methyl-2-pyrrolidone were distilled prior to use.

Cyclic Voltammetry. Electrochemical experiments were performed with a VMP3 (BioLogic Science Instruments) potentiostat in an airtight electrochemical cell (Gamry Instruments). The latter consisted of a traditional three-electrode system utilizing a Ag wire as the pseudoreference electrode, which was calibrated with respect to the potential of the Fc^+/Fc redox couple, and platinum wire as the counter electrode. The cell also had inlet and outlet valves for oxygen or argon purging. The glassy carbon (3 mm diameter) working electrode was polished with 0.05 mm alumina paste prior to the experimentation. The cell was assembled in an Ar atmosphere glovebox where H_2O and O_2 concentrations were kept below 1 ppm. The supporting electrolyte salts, tetrabutylammonium perchlorate (TBAP) and tetrabutylammonium bis(trifluoromethane)sulfonimide (TBATFSI), were received from Sigma-Aldrich and dried under vacuum at 50 °C for 12 h prior to use. All solutions were prepared in the glovebox by dissolving 0.1 mol/L TBA salt in the desired solvent. The electrolyte solutions were first purged with argon, and the electrode was cycled continuously until a reproducible cyclic voltammetric profile was obtained. The solutions were then purged with O_2 for ORR measurements. All experiments were performed at room temperature.

Gas Chromatography−Mass Spectrometry. GCMS tests were performed with an Agilent Technologies 7820A gas chromatograph coupled with an Agilent Technologies 5975 mass spectroscopy detector. A typical run utilized a 1 μL injection volume and He gas flow rate of 1.2 mL/min. Samples for analysis were prepared in an Ar glovebox by combining 30 μL of the solvent to be analyzed in 30 mL of anhydrous acetonitrile. Next, 5 mL of the solvent mixture was added to enough $KO_2^•$ in a screw cap vial to make a 0.5 M solution. For samples that passed the initial $KO_2^•$ test, a separate run was included where a spatula tip of 18-crown-6 ether was added to the 0.5 M $KO_2^•$ solution. Finally, each vial was closed tightly and covered in parafilm. Measurements were taken after 1 day and 1 week, and the signals were compared against a blank. Potassium superoxide ($KO_2^•$, 96.5%, Alfa Aesar) and 18-crown-6 (99%, Sigma-Aldrich) were used as received. Water content was below 40 ppm for all GCMS experiments, as determined by Karl Fischer titration using a Mettler-Toledo coulometer.

RESULTS

Quantum Chemical Investigation of Solvent Reactivity. In this work, we combine density functional theory (B3LYP) with the Poisson−Boltzmann continuum solvent model to predict the reactivity of aprotic solvents in the nucleophilic substitution reactions with the superoxide anion radical. This provides a theoretical framework for computational screening of stable aprotic solvents for Li−air batteries. We have investigated a wide spectrum of aprotic solvents employed or tested in Li and Li ion batteries, such as organic cyclic and linear carbonates, sulfonates, aliphatic and aromatic carboxylic esters, lactones, *N*-alkyl amides, lactams, phosphinates, phosphonates, phosphates, sulfones,

Table 2. Computed Free Energy Barriers (ΔG_{act}) and Reaction Free Energies (ΔG_r) for Nucleophilic Reactions of Superoxide Ion in the Implicit Solvent Reaction Field (kcal/mol)

	solvent/substrate	structure	carbon site[a]	ε (solvent)[b]	ΔG_{act}	ΔG_r
			1, C_5	64.4	15.47	-5.64
1	PC	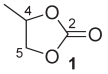	**1**, C_4	64.4	16.75	-5.49
			1, C_2	64.4	41.85	36.93
2	EC		**2**, C_4	89.6	14.22	-6.94
3	DMC	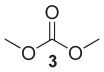	**3**, CH_3–	3.09	12.42	-11.39
4	Me-Tos	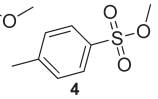	**4**, CH_3–(O)	36.0 (MeCN)	10.17	-19.06
			5, C_4	39.1	16.52	-4.99
5	GBL		**5**, C_3	39.1	54.61	35.81
			5, C_1	39.1	31.71	18.71
6	GVL	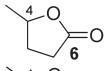	**6**, C_4	39.1 (GBL)	18.26	-3.84
7	4,4-diMe-GBL	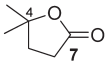	**7**, C_4	39.1 (GBL)	20.16	-1.15
8	4,4-diF-GBL	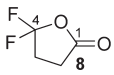	**8**, C_4	39.1 (GBL)	27.41	-1.01
			8, C_1	39.1 (GBL)	6.95	3.24
9	MeOAc		**9**, CH_3–(O)	36.0 (MeCN)	19.25	-1.30
			9, >C=O	36.0 (MeCN)	34.64	27.21
10	PhB	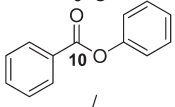	**10**, >C=O	36.0 (MeCN)	14.45	0.91
			11, C_5	32.2	40.18	25.59
11	NMP		**11**, C_3	32.2	61.30	38.03
			11, C_2	32.2	43.74	23.74
12	TMP	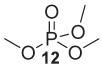	**12**, CH_3–	36.0 (MeCN)	12.55	-13.59
13	DMMP		**13**, CH_3–(O)	36.0 (MeCN)	14.37	-10.45
14	MDMP		**14**, CH_3–(O)	36.0 (MeCN)	17.63	-6.55
15	EMS		**15**, CH_3–(S)	95.0	22.79	2.79
16	SFL		**16**, CH_2–(S)	90.0	20.19	-2.98
17	MeCN	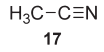	**17**, -CN	36.0	24.92	18.96
			17, CH_3–	36.0	42.70	20.56
18	BN	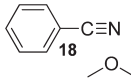	**18**, -CN	25.2	25.31	21.57
19	DME	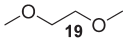	**19**, CH_3–	7.2	31.56	19.88

[a] The carbon site of nucleophilic attack by superoxide. [b] Solvent dielectric constant.

nitriles, and ethers. It should be noted that the initial nucleophilic displacement reaction involving superoxide is typically the rate-determining step. A subsequent one-electron reduction of organic peroxy radicals by O_2^- to peroxy anions and their further reactions to form stable oxidation products (see Scheme 1 for an example) is highly exergonic and occurs near the diffusion-controlled limit.[31,54−56] Therefore, the theoretical analysis of solvent reactivity is restricted to the initial rate-limiting nucleophilic attack of superoxide on organic solvents. Computed free energy barriers (ΔG_{act}) and reaction free energies (ΔG_r) for reactions of $O_2^{\bullet-}$ with 19 organic solvents are summarized in Table 2. In several instances we report the results for several possible reaction sites in a solvent molecule, which provide a detailed mechanistic understanding of the relevant reaction pathways of solvent decomposition. The theoretical predictions for a number of commercially available solvents are consistent with the solvent stability tests performed by cyclic voltammetry and GCMS (see below), thus supporting the validity of the computational approach adopted in this paper. We find that the solvents with ΔG_{act} < 20 kcal/mol are chemically unstable against $O_2^{\bullet-}$. Conversely, the solvents with ΔG_{act} > 24 kcal/mol do not show appreciable reactivity with superoxide and,

dx.doi.org/10.1021/jp2073914 |J. Phys. Chem. A 2011, 115, 12399–12409

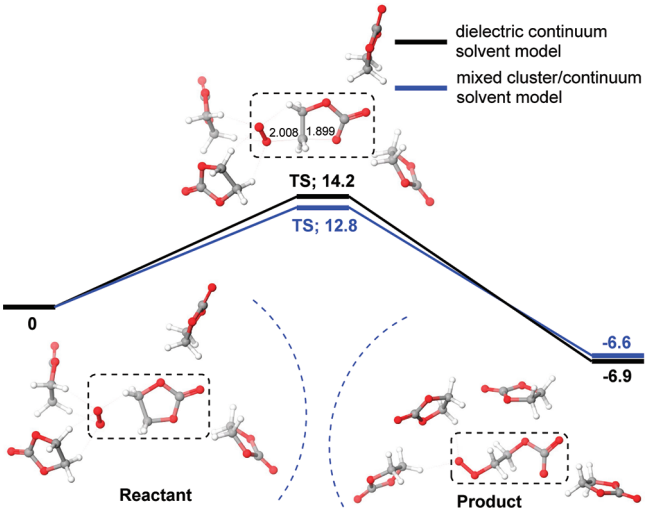

Figure 2. Comparison of reaction free energy profiles (T = 298.15 K) for superoxide addition to the etheral carbon atom of ethylene carbonate calculated using a pure dielectric continuum solvent model (the structures of reacting molecules are shown inside a dashed box) and a mixed cluster/continuum representation of the solvent by inclusion of four additional solvent molecules (kcal/mol).

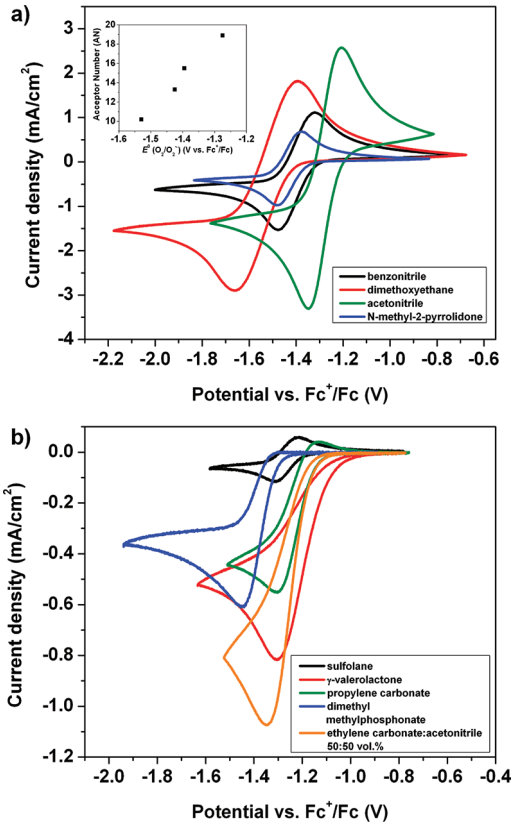

Figure 3. IR-corrected cyclic voltammograms of oxygen reduction at a glassy carbon disk electrode (scan rate, 50 mV/s; supporting electrolyte, 0.1 M TBAP except for dimethoxyethane that used TBATFSI in similar concentration) in (a) benzonitrile, dimethoxyethane, acetonitrile, and *N*-methyl-2-pyrrolidone and (b) sulfolane, γ-valerolactone, propylene carbonate, dimethyl methylphosphonate, and 50:50 vol % ethylene carbonate:acetonitrile solvents. (inset) Correlation between the solvent acceptor number (AN) and the formal potential (E^0) for $O_2/O_2^{\bullet-}$ redox couple.

therefore, serve as candidate electrolyte solvents for Li−air batteries.

Cyclic Voltammetry Study of Solvent Reactivity. Cyclic voltammetry (CV) is a well-known technique extensively used to study the reversibility of electrochemical reactions.[22,39−42] One parameter of interest on these i−E curves is the ratio of anodic and cathodic peak currents. A ratio of unity produces symmetrical cyclic voltammograms as the electrogenerated product is stable and can undergo a reversible electrochemical reaction. One can therefore apply such a technique to qualitatively assess the reactivity of a given electrochemical species (e.g., $O_2^{\bullet-}$) as a function of solvent or electrode material type.[14] In the present analysis, a solvent is deemed a pass according to the cyclic voltammetry test if the ratio of anodic to cathodic peak currents appears to be unity. It is however worth noting that, under these conditions, the electrolyte is exposed to superoxide anions on the time scale of only a few minutes. Subsequent longer exposure chemical tests are required to further verify the stability of our solvents, and for that purpose, the GCMS experiments were run in parallel.

The electroreduction of oxygen in aprotic media and in the presence of quaternary ammonium salts (e.g., Bu_4NClO_4) leads to the formation of superoxide radical anion. Full reversibility of the $O_2/O_2^{\bullet-}$ couple is indicative of the chemical stability of the electrogenerated $O_2^{\bullet-}$ and hence the nonreactivity of solvent molecules with $O_2^{\bullet-}$ over the time scale of the scan. In contrast, a decrease or complete suppression of the reverse anodic peak current is a strong indication of a fast chemical reaction between superoxide and a solvent molecule.

Figure 3 shows cyclic voltammograms (CVs) at a glassy carbon disk electrode with oxygen saturation in several commercially available solvents with 0.1 M TBAP at scan rate of 50 mV/s. Voltammetric results obtained at varying scan rates (5−100 mV/s) are shown in Figures 1S−9S in the Supporting Information. Within the time scale of a typical electrochemical test, benzonitrile, dimethoxyethane, acetonitrile, and *N*-methyl-2-pyrrolidone solvents are stable when superoxide anions are formed upon reduction of oxygen. On the other hand, sulfolane, γ-valerolactone, propylene carbonate, dimethyl methylphosphonate, and 50:50 vol % ethylene carbonate:acetonitrile solvents are unstable in the presence of the free radical. The inset in Figure 3a emphasizes the effect of solvent properties on the formal potential (E^0) for the $O_2/O_2^{\bullet-}$ redox couple, the latter being more positive as the solvent acceptor number[57] increases, which is consistent with a stronger solvation medium for the superoxide anion.[39] Table 3 lists qualitative pass/fail results, and Table S1 in the Supporting Information summarizes peak current ratios, formal potentials for the $O_2/O_2^{\bullet-}$ redox couple, and acceptor numbers for the stable candidate solvents presented in Figure 3a. The peak current ratio for these solvents is close to unity at a sweep rate as slow as 5 mV/s.

Gas Chromatography−Mass Spectrometry Study of Solvent Reactivity. GCMS analysis was used as a quick screening technique to determine if solvents are stable to $KO_2^{\bullet}$, as a chemical source of superoxide radicals. By allowing dilute solutions of the solvents to react with relatively large quantities of $KO_2^{\bullet}$, a qualitative pass/fail assessment can be determined regarding solvent stability by monitoring changes in solvent chromatographic peaks. Solvents were submitted to a series of increasingly rigorous tests for stability. A solvent was deemed

Table 3. Comparison of Qualitative GCMS and CV Results on Solvent Stability with Theoretical Predictions Based on Computed Free Energy Barriers (ΔG_{act}) for Nucleophilic Substitution by Superoxide (kcal/mol)

solvent	GCMS[a]	CV[b]	ΔG_{act}[c]
EC	fail	fail[d]	14.22
DMMP	fail	fail	14.37
PC	fail	fail	15.47
GVL	fail	fail	18.26
SLF	pass	fail	20.19
MeCN	NA[e]	pass	24.92
BN	fail[f]	pass	25.31
DME	pass	pass	31.56
NMP	pass	pass	40.18

[a] A pass indicates that the signal from the reaction mixture has roughly the same integration as the blank for that solvent, while a fail indicates a significant loss of signal. [b] A pass indicates that the ratio of anodic to cathodic peak currents is close to unity, while a fail indicates a significant deviation from unity (Figure 3). [c] The computed data are taken from Table 2. [d] A 1:1 v/v EC/MeCN mixture. [e] A rigorous assessment of solvent loss cannot be made for the carrier solvent. [f] OH^- present in $KO_2^\bullet$ (96.5% pure) is likely to be the reactive species responsible for the decomposition of nitrile solvents.

a "pass" only if the solvent chromatographic peaks did not change appreciably after 1 week of storage with $KO_2^\bullet$ and 18-crown-6 ether. The crown ether was included in order to enhance the dissociation of $KO_2^\bullet$, particularly for solvents with lower dielectric constants. In order to observe clearly discernible changes in chromatographic peaks, each solvent of interest needed to be diluted with a carrier solvent. Acetonitrile was selected as a carrier solvent due to the ease of obtaining clear chromatographic peaks for the solvents under examination in its presence. The results of the GCMS screening of stable solvents are summarized in Table 3, where they are compared with qualitative results obtained by cyclic voltammetry and theoretical predictions based on computed free energy barriers for nucleophilic substitution by superoxide. A detailed account of the results is provided in Table S3 and Figure S10 in the Supporting Information.

DISCUSSION

For clarity, each class of solvents is discussed in a separate section below following the same order: the most favorable reaction pathway of decomposition by superoxide, the possibility of alternative reaction routes, and the comparison of the theoretical predictions with available experimental data. Views of transition state and product geometries for selected solvents are provided in the corresponding sections below.

Organic Carbonates. We have previously[23] investigated possible mechanisms of superoxide-induced decomposition of carbonate-based electrolytes, so only a brief account of the computational results will be given here. Results of reaction path modeling suggested a mechanism in which $O_2^{\bullet-}$ easily attacks the etheral carbon atom of carbonate solvents as shown in Figure 1. Calculated activation energies follow the order 12.4 (DMC) < 14.2 (EC) < 15.5 (PC), in line with larger exothermicity and stronger electrophilic character of the *O*-alkyl carbon. Based on the electrophilicity or positive atomic charge alone (Table S2 in the Supporting Information), nucleophilic substitution at the carbonyl carbon would be most reasonable.[16−18] However, this conjecture is not supported by our calculations. We find that $O_2^{\bullet-}$ addition to the carbonyl carbon of PC leads to an adduct that is 36.9 kcal/mol less stable than the reactant complex and requires an activation energy of 41.9 kcal/mol (Table 2).

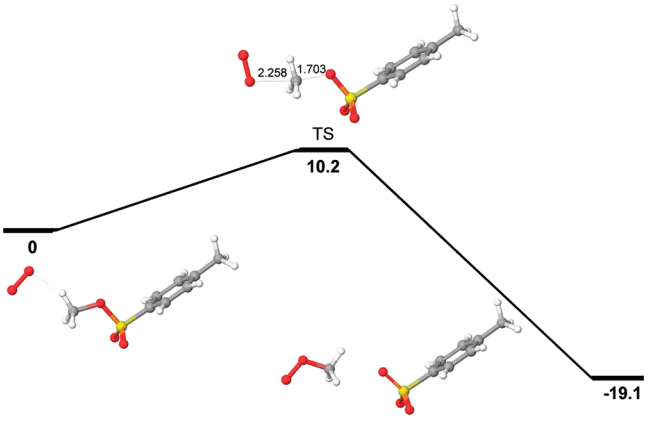

Figure 4. Reaction free energy profile for nucleophilic attack of $O_2^{\bullet-}$ at the etheral carbon atom of methyl tosylate calculated in the field of continuum solvent (kcal/mol). B3LYP optimized C−O bond lengths in the transition state are shown.

Figure S1 in the Supporting Information shows the CVs of oxygen reduction in PC and 1:1 v/v EC/MeCN (+0.1 M TBAP) as a function of scan rate. EC is solid at room temperature and needs to be mixed with another solvent, in which the oxygen reduction process is completely reversible (e.g., acetonitrile, Figure 3a and Figure S7 in the Supporting Information). On the other hand, DMC + 0.1 M TBAP electrolyte is not sufficiently conductive to permit reliable electrochemical measurements. It is seen that the reduction in 1:1 v/v EC/MeCN is totally irreversible, because the reoxidation wave of $O_2^{\bullet-}$ is entirely absent in the voltage scan rate range of 5−100 mV/s. In contrast, the voltammetry in PC reveals the presence of some $O_2^{\bullet-}$ oxidation peak at 100 mV/s, which becomes progressively smaller as the sweep rate decreases and completely disappears at 10 mV/s. The loss of $O_2^{\bullet-}$ observed by CV is consistent with relatively low kinetic barriers predicted for reactions of PC and EC with $O_2^{\bullet-}$. The relative stability of $O_2^{\bullet-}$ in these two solvents is also nicely reproduced by the calculations. Finally, the results of GCMS tests are in agreement with theoretical predictions and electrochemical measurements, indicating that PC and EC are unstable in the presence of excess $KO_2^\bullet$ in acetonitrile and completely react within 7 days.

Sulfonate Esters. The reactivity of superoxide with alkyl sulfonates has been well studied in the past.[28,57] This example can be used to demonstrate the predictive value of our applied computational methodology. The reaction free energy profile for the nucleophilic attack of $O_2^{\bullet-}$ on the *O*-alkyl carbon atom of methyl tosylate is shown in Figure 4. The results of calculations indicate that this is a very fast reaction, with the lowest activation free energy and the most negative reaction free energy among those listed in Table 2. The possibility of $O_2^{\bullet-}$ addition to the sulfur atom can be excluded, because this would lead to a peroxide intermediate lying 25.9 kcal/mol above the reactant complex. The present calculations are in full agreement with the experimental results[57] describing the reaction of superoxide with alkyl tosylates as an extraordinarily rapid process proceeding by an S_N2 type mechanism with inversion of configuration.

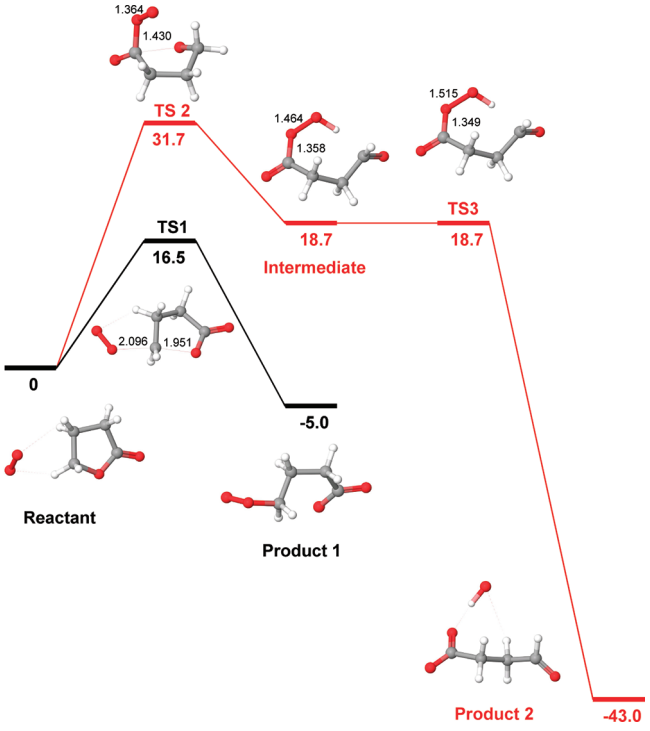

Figure 5. Reaction free energy profiles for nucleophilic attack of $O_2^{\bullet-}$ at the etheral (gray) and carbonyl (red) carbon atoms of γ-butyrolactone calculated in the field of continuum solvent (kcal/mol). B3LYP optimized bond lengths are shown.

Aliphatic Esters and Lactones. Figure 5 represents reaction free energy profiles of the nucleophilic attack by $O_2^{\bullet-}$ on the two potential reaction sites in γ-butyrolactone. As in the case of organic carbonate solvents, superoxide addition to the etheral carbon atom is the most kinetically favorable process with a transition state lying 16.5 kcal/mol above the reactant complex. An alternative reaction pathway involving the addition of $O_2^{\bullet-}$ to the carbonyl carbon requires a considerably higher activation energy (31.7 kcal/mol), which might not be easily accessible at room temperature. Once this transition state is reached, however, there is a remarkably high thermodynamic driving force to form highly unstable acyl hydroperoxide anion radical that undergoes nearly barrierless O—O bond homolysis to yield $^{\bullet}OH$ and $^{-}OOCCH_2CH_2CHO$.

Methyl acetate shows a qualitatively similar behavior in its reactivity with superoxide. *O*-Alkyl cleavage associated with the nucleophilic displacement of the carboxylate ion (ΔG_{act} = 19.3 kcal/mol) is highly favored over carbonyl carbon—oxygen cleavage associated with the displacement of the methoxy radical (ΔG_{act} = 34.6 kcal/mol).

The described mechanism of superoxide-induced decomposition of lactones and aliphatic esters is confirmed in the gas phase, as evidenced by mass spectrometric studies (path a in Scheme 2).[37,38] In particular, experiments with $^{18}O_2^{\bullet-}$ showed no evidence for ^{18}O incorporation into the carboxylic moiety, establishing that S_N2 displacement at the *O*-alkyl group is the only observable reaction channel.[38] Conversely, liquid-phase reactions of $O_2^{\bullet-}$ with aliphatic esters are generally assumed to proceed via attack at the carbonyl carbon, followed by displacement of an alkoxy anion (path c in Scheme 2).[28,34−36] In fact, path c is the least likely from the computational viewpoint, because it is thermodynamically

Scheme 2. Three Possible Mechanisms for the Initial Reaction of Superoxide with Methyl Esters of Carboxylic Acids[a]

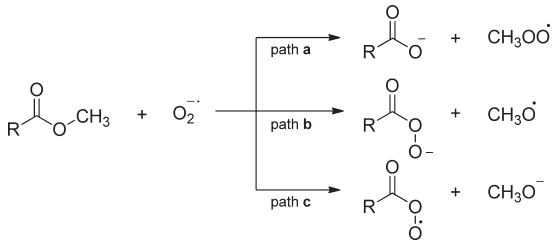

[a] Path a is supported by the current DFT calculations.

much less favorable than path b involving the homolytic scission of the acyl—oxygen bond and formation of an alkoxy radical (for CH_3COOCH_3, the difference is ~19 kcal/mol in the gas phase and ~9 kcal/mol in acetonitrile solution). An important argument in support of path c has been that the reaction of $KO_2^{\bullet}$-18-crown-6 with (*R*)-$CH_3CO_2CH(CH_3)C_6H_{13}$ in benzene yields (*R*)-2-octanol with retention of configuration at the stereogenic center.[34] However, the interpretation of some $KO_2^{\bullet}$ experiments may be complicated by the presence of various admixtures in $KO_2^{\bullet}$ (KOH, K_2O_2, and K_2CO_3 being the main impurities) and accumulation of decomposition products in $KO_2^{\bullet}$ solution that can change the course of the reaction.[35,58,59] As a matter of fact, KOH under similar conditions to $KO_2^{\bullet}$ is able to induce the acyl—oxygen fission in alkyl esters with retention of configuration.[34,60] Additional experiments with the electrochemically generated superoxide are needed to verify the results obtained in the reactions of esters with $KO_2^{\bullet}$.

The reactivity of alkyl esters with $O_2^{\bullet-}$ can, in principle, be modified through the addition of substituents at the etheral carbon. To elucidate the magnitude of such substituent effects, we have examined a series of γ-lactones with 4-methyl, 4,4-dimethyl, and 4,4-difluoro groups. The addition of one and two alkyl groups increases the activation free energy by 1.7 and 3.6 kcal/mol, respectively (Table 2). This is to be expected because the addition of each methyl group to the reactive site makes it more sterically hindered and less electrophilic. However, the stabilizing effect is relatively small and will not preclude solvent decomposition.

Perhaps the most striking is the ability of fluorine atoms attached to the *O*-alkyl carbon to change a mode of the reaction between superoxide and aliphatic lactones (Figure 6). On the one hand, the activation energy for nucleophilic attack at the etheral carbon is increased significantly from 16.5 to 27.4 kcal/mol. We ascribe this effect to the increased repulsion between $O_2^{\bullet-}$ and fluorine atoms and the enhanced strength of the CF_2—O bond,[61] which is 0.055 Å shorter than that in the nonfluorinated analogue. On the other hand, the reaction barrier for the attack at the carbonyl carbon is decreased dramatically from 31.7 to 6.9 kcal/mol, making 4,4-difluoro-γ-butyrolactone extremely unstable in the presence of superoxide. This can be attributed to the formation of a rather stable alkoxy anion in which the negative charge is delocalized by the strong electron-withdrawing fluorine groups. We expect that α-fluorinated lactones will also be susceptible to nucleophilic attack at the electrophilically activated carbonyl carbon, as has been reported[37] previously for alkyl esters of trifluoroacetic acid.

Cyclic voltammetry curves for reduction of oxygen to $O_2^{\bullet-}$ in γ-valerolactone containing TBAP are shown in Figure S3 in the

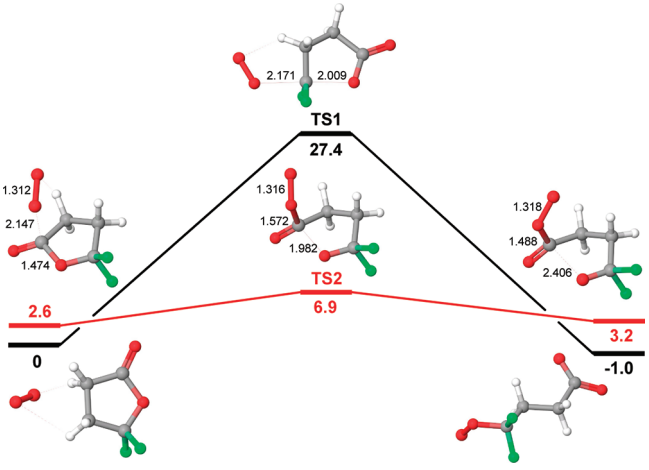

Figure 6. Reaction free energy profiles for nucleophilic attack of O_2^- at the etheral (gray color) and carbonyl (red color) carbon atoms of 4,4-difluoro-γ-butyrolactone calculated in the field of continuum solvent (kcal/mol). B3LYP optimized bond lengths are shown.

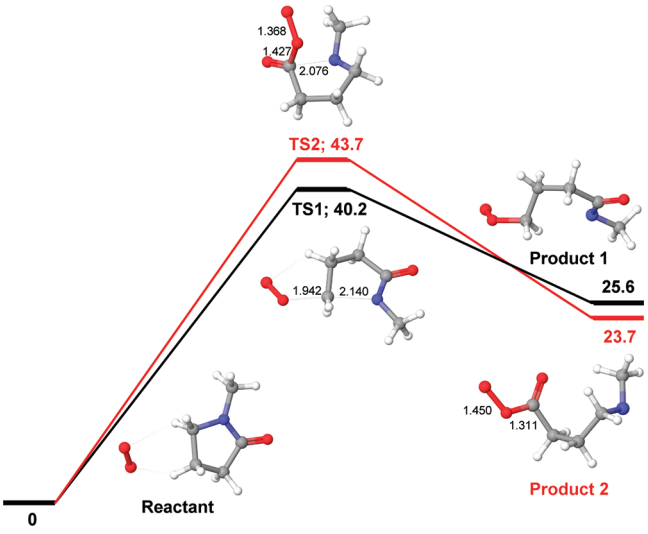

Figure 7. Reaction free energy profile for nucleophilic attack of O_2^- at the etheral (gray) and carbonyl (red) carbon atoms of *N*-methyl-2-pyrrolidone calculated in the field of continuum solvent (kcal/mol). B3LYP optimized bond lengths are shown.

Supporting Information. The anodic peak of the $O_2^{\bullet-}/O_2$ couple is absent even at the highest sweep rate of 100 mV/s. This result is consistent with a rapid decomposition of $O_2^{\bullet-}$ in γ-lactones. Furthermore, fast solvent oxidation is confirmed by gas chromatographic tests carried out using a large access of $KO_2^{\bullet}$ in acetonitrile and by analyzing the reaction products using in situ generated $Et_4N^+O_2^{\bullet-}$ in dimethylformamide.[62]

Aryl Benzoates. In contrast to alkyl esters, the possibility of S_N2 attack resulting in the cleavage of the *O*-aryl bond in aromatic esters is generally precluded.[38,63,64] Thus, the nucleophilic addition to phenol esters proceeds exclusively at the carbonyl center. The reaction rate is typically much faster than that of the corresponding alkyl esters.[34,35] These experimental results are corroborated by our quantum chemical calculations (Table 2). Indeed, the reaction of $O_2^{\bullet-}$ with phenyl benzoate proceeds via attack on the carbonyl carbon, followed by displacement of the phenolate ion. The activation barrier for this process is only 14.5 kcal/mol, which is 4.8 kcal/mol lower than that for methyl acetate.

***N,N*-Dialkyl Amides and *N*-Alkyl Lactams.** Although we restrict our discussion to *N*-methyl-2-pyrrolidone (NMP) in this section, other *N*-alkyl substituted amides are expected to behave similarly. In contrast, primary and secondary amides having somewhat acidic hydrogen atoms (pK_a of 25−26 in DMSO[65,66]) may be slowly oxidized by $O_2^{\bullet-}$ via initial proton transfer. The results shown in Table 2 and Figure 7 suggest that nucleophilic substitution at any ring carbon atom is improbable, since the calculated energy barriers are high (ΔG_{act} = 40.2−43.7 kcal/mol) and the first reaction step is significantly uphill in free energy (ΔG_r = 23.7−25.6 kcal/mol). Such contrasting behavior of amides with respect to esters can be rationalized on the basis of the relative stability of reaction products, namely, amide and carboxylate anions. The computational results are consistent with our results from cyclic voltammetry and GCMS. The voltammetry peaks for the reduction of oxygen in NMP remain highly symmetric down to the lowest potential scanning rate (Figure S4 in the Supporting Information). Similarly, the NMP signal from the GCMS analysis is largely unaffected by $KO_2^{\bullet}$ after 7 days of treatment.

Phosphinates, Phosphonates, and Phosphates. In this section we examine the nucleophilic reactivity of methyl esters of phosphinic, phosphonic, and phosphoric acids. The computational data reported in Table 2 indicate that $O_2^{\bullet-}$ is able to carry out a nucleophilic attack on the *O*-alkyl carbon of phosphorus(V) esters in the same way as was found for alkyl esters of carboxylic acids. These reactions are predicted to be 6.6−13.6 kcal/mol exothermic and have activation energies in the range 12.6−17.6 kcal/mol. The calculated sequence of the activation and reaction energies is found to be as follows: phosphinate (MDMP) > phosphonate (DMMP) > phosphate (TMP), which correlates with the larger basicity of the displaced anion. An alternative mechanism involving a nucleophilic attack on the phosphorus atom is unlikely. This assertion is based on the relative energy of a peroxyphosphate intermediate, which is 29.4 kcal/mol less stable than the initial TMP−$O_2^{\bullet-}$ complex. Voltammograms of oxygen-saturated DMMP show a significant asymmetry between the reduction and reoxidation processes (Figure S5 in the Supporting Information), indicating that the electrogenerated superoxide undergoes a fast chemical reaction with the substrate. Furthermore, DMMP shows appreciable reactivity with $KO_2^{\bullet}$, further supporting our theoretical results.

Alkyl Sulfones. To extend our understanding of superoxide reactivity toward non-ester organic substrates, we have investigated ethyl methyl sulfone (EMS) and sulfolane (SFL) solvents. We find that the most plausible pathway for the reaction between $O_2^{\bullet-}$ and sulfones is a nucleophilic attack at the C_α atom, followed by C−S bond cleavage to give a sulfinate anion (Figure 8). Again, the reaction is driven by the formation of a fairly stable anion with a delocalized charge. Although the thermodynamics and kinetics of this process are not as favorable as for esters of organic and inorganic acids, it is still expected to occur at standard conditions, though at a slower rate. This conclusion is fully supported by cyclic voltammetry experiments. The anodic to cathodic peak current ratio of the $O_2^{\bullet-}/O_2$ couple in SFL is close to unity only at the sweep rate of 100 mV/s (Figure S6 in the Supporting Information). Decreasing the sweep rate causes a faster decrease in the anodic current due to chemical reaction involving the consumption of $O_2^{\bullet-}$. Analysis of the GCMS chromatogram of sulfolane at 1 week revels that both tests with $KO_2^{\bullet}$ have lower

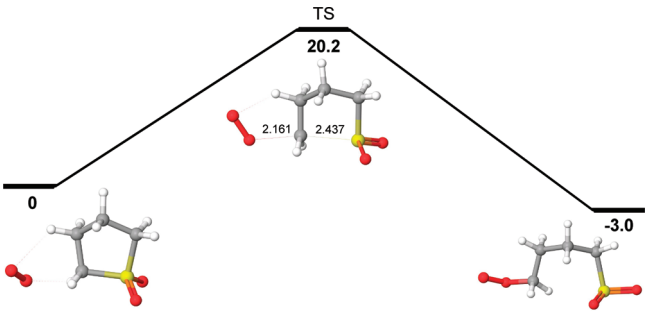

Figure 8. Reaction free energy profile for nucleophilic attack of O_2^- at the C_α atom of sulfolane calculated in the field of continuum solvent (kcal/mol). B3LYP optimized C−O bond lengths in the transition state are shown.

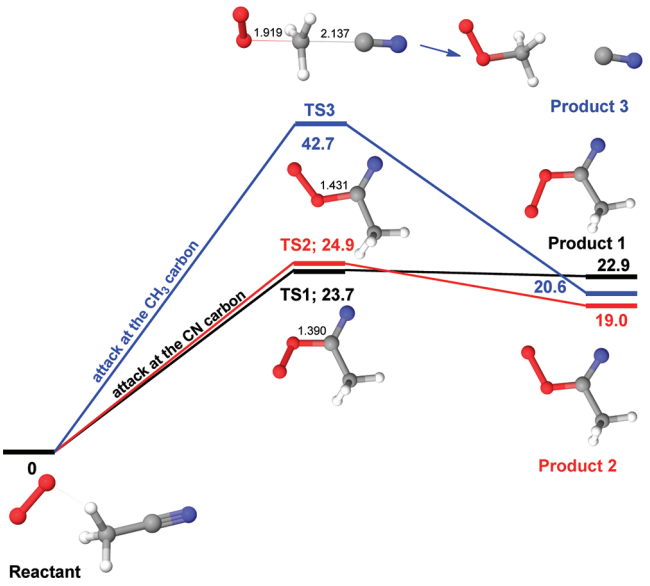

Figure 9. Reaction free energy profile for nucleophilic attack of O_2^- at the CN (two different configurations in gray and red) and CH_3 (blue) carbon atoms of acetonitrile calculated in the field of continuum solvent (kcal/mol). B3LYP optimized bond lengths are shown.

peak areas than the blank sample. However, the differences in areas are not outside the experimental error generated by sample injections of the machine and slight differences in evaporation of samples stored over 1 week.

Aliphatic and Aromatic Nitriles. Reaction free energy profiles for superoxide addition to the methyl and cyano carbon atoms of acetonitrile (MeCN) are shown in Figure 9. Nucleophilic addition at the CN carbon proceeds with an activation energy of 23.7−24.9 kcal/mol and gives an adduct that lies 19.0−22.9 kcal/mol above the reactant complex. In contrast to alkyl esters, subsequent one-electron reduction of $^{\bullet}N{=}C(OO^-)CH_3$ by $O_2^{\bullet-}$ is slightly endergonic (ΔG_r = 1.6 kcal/mol) and requires an additional activation energy to overcome the Coulomb repulsion between the two anions. Nucleophilic substitution at the CH_3 carbon is even less likely to occur since the activation energy for this process is prohibitively high at room temperature (ΔG_{act} = 42.7 kcal/mol). Relatively high activation barriers for nucleophilic reactions of $O_2^{\bullet-}$ with MeCN agree with the cyclic voltammetry results, indicating that the oxygen

Scheme 3. Base-Catalyzed Self-Condensation of Acetonitrile

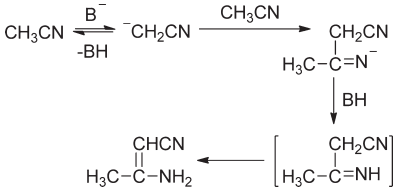

reduction process in MeCN is fully reversible. This is consistent with previous observations that relatively stable solutions of $O_2^{\bullet-}$ can be obtained in MeCN by electrochemical methods.[39,67,68] Conversely, when $KO_2^{\bullet}$ (only 96.5% pure) with 18-crown-6 ether or impure $[(Me_4N)O_2]$ (contaminated with OH^-) is used as source of superoxide in MeCN, a slow reaction with the solvent is reported.[68,69] Small yields of acetamide were identified by gas liquid chromatography[69] and absorption spectroscopy.[68] Interestingly, an analogous absorption spectrum develops when KOH is added to electrogenerated $O_2^{\bullet-}$,[68] indicating that OH^- is likely to be the reactive species responsible for the attack at the CN carbon. In addition, a small amount of 3-aminocrotononitrile is observed in the present GCMS experiments, when either $KO_2^{\bullet}$ or KOH is added to anhydrous MeCN. Base-mediated self-condensation of acetonitrile to form 3-aminocrotononitrile (Thorpe reaction)[70] is outlined in Scheme 3.

Nucleophilic reactivity of benzonitrile (BN)[34,71] is similar to that of MeCN (Table 2 and Figure 3a). BN and MeCN have comparable activation energies for the addition of $O_2^{\bullet-}$ to the CN carbon, which are sufficiently high to exclude the possible chemical reaction with electrogenerated $O_2^{\bullet-}$, at least on the time scale of voltammetry (Figures S7 and S8 in the Supporting Information). However, both BN[34] and MeCN[69,70] are slowly decomposed during the $KO_2^{\bullet}$ or KOH treatment.

Glymes. The ether functionality is not expected to be susceptible to nucleophilic attack.[19,72] The results of calculations (Table 2) confirm that a nucleophilic substitution reaction between dimethoxyethane (DME) and superoxide is strongly unfavorable under standard conditions (ΔG_{act} = 31.6 kcal/mol; ΔG_r = 19.9 kcal/mol). This is further corroborated by the stability of the electrochemically generated superoxide in DME (Figure S8 in the Supporting Information) and no detectable decomposition of DME and triglyme in the presence of $KO_2^{\bullet}$.

SUMMARY AND CONCLUSIONS

A wide spectrum of aprotic organic solvents has been tested as electrolyte components in Li ion batteries.[73] The most promising classes that qualify as advantageous electrolyte solvents or cosolvents have been considered as a part of electrolyte composition for the nonaqueous Li−air battery. However, recent experimental results[14−21] strongly suggest that cyclic and linear carbonates, commonly used electrolytes in commercial Li ion batteries, are unstable against superoxide, the one-electron reduction product of oxygen. Since then, understanding the factors influencing solvent instability and identification of appropriate electrolyte compositions for Li−air systems has drawn tremendous research attention.

In this study, we have used quantum chemical calculations to investigate the reactivity of a number of aprotic electrolyte solvents in nucleophilic substitution reactions with superoxide. Theoretical calculations have been complemented by cyclic

voltammetry to study the electrochemical reversibility of the $O_2^{\bullet-}/O_2$ couple in commercially available aprotic solvents containing a TBA salt and GCMS measurements to monitor solvent stability using $KO_2^{\bullet}$ as a chemical source of superoxide. Excellent agreement between the theoretical predictions and both experimental sets of data has been achieved in evaluating solvent reactivity with superoxide. This serves as a validation of both computational and experimental methods as powerful screening techniques to identify suitable solvents for Li−air battery applications.

This study has refined our understanding of solvent instability in the nucleophilic substitution reactions with superoxide. We find that the nucleophilic attack of $O_2^{\bullet-}$ at the *O*-alkyl carbon is a common mechanism of decomposition of organic carbonates, sulfonate esters, aliphatic carboxylic esters, lactones, sulfones, and alkyl esters of phosphinic, phosphonic, and phosphoric acids. In contrast, nucleophilic reactions of $O_2^{\bullet-}$ with phenol esters of carboxylic acids and *O*-alkyl fluorinated aliphatic lactones proceed via attack at the carbonyl carbon. We were also able to identify chemical functionalities stable against nucleophilic substitution by superoxide. These include *N*-alkyl substituted amides, lactams, nitriles, and ethers (glymes). Nitriles, however, slowly react, when treated with strong bases (i.e., KOH). The results clearly indicate that solvent reactivity (ΔG_{act}) is strongly correlated to the thermodynamic stability of the reaction products (ΔG_r) (correlation coefficient of 0.899). The lower the basicity of the displaced anion (the stronger the conjugate acid), the higher is the reactivity of an organic substrate in nucleophilic substitution reactions with superoxide. However, we find no significant correlation between the activation free energy, ΔG_{act}, and simple molecular descriptors of chemical reactivity, such as atom-centered Mulliken charges, electrostatic potential derived charges, and nucleophilic Fukui functions (Table S2 in the Supporting Information).[74] These indices alone cannot be used to predict accurately either a position for nucleophilic attack or the magnitude of the activation energy.

The current study has established that the nucleophilic addition of $O_2^{\bullet-}$ to alkyl esters occurs at the *O*-alkyl carbon, whereas the nucleophilic addition to phenol esters proceeds at the carbonyl center. This is in agreement with the nucleophilic reactivity of $O_2^{\bullet-}$ in the gas phase, as evidenced by several mass spectrometry studies.[37,38] Conversely, only the attack on the carbonyl carbon has been generally assumed for both alkyl and aryl esters in aprotic solvents.[28,34−36] Based on the drastically different activation energies for the two reaction pathways, nucleophilic substitution at the carbonyl carbon of aliphatic esters is not supported by our calculation.

Despite their successful use in Li ion batteries, simple organic esters of carbonic, carboxylic, and several inorganic acids are found to be unstable against superoxide and cannot be used in the Li−air battery. Knowledge and a detailed understanding of the reaction mechanisms provide an important basis for the selection and design of stable electrolyte systems. One unexplored strategy to enhance solvent stability could conceivably be through the introduction of bulkier substituents for steric protection of the reactive site. The current study represents only one aspect of solvent reactivity, that is, nucleophilic substitution by superoxide. It is likely, however, that some candidate solvents may be sensitive to molecular oxygen, or could be oxidized by superoxide via initial proton abstraction or electron transfer. Some of these aspects of solvent reactivity will be the scope of our future work.

■ ASSOCIATED CONTENT

Supporting Information. Complete ref 44, formal potentials for the $O_2/O_2^{\bullet-}$ redox couple, peak current ratios, and acceptor numbers for the stable solvents (Table S1), computed atomic charges and nucleophilic Fukui indices for solvent molecules (Table S2), cyclic voltammograms of oxygen reduction at a glassy carbon disk electrode in aprotic solvents at different scan rates (Figures S1−S9), and solvent chromatographic peaks from the GCMS analysis (Table S3, Figure S10). This material is available free of charge via the Internet at http://pubs.acs.org.

■ AUTHOR INFORMATION

Corresponding Author

*E-mail: slava@liox.com.

Present Addresses

[†]Materials and Process Simulation Center, Beckman Institute 139-74, California Institute of Technology, Pasadena, CA, 91125, United States.

■ REFERENCES

(1) Abraham, K. M.; Jiang, Z. A. *J. Electrochem. Soc.* **1996**, *143*, 1–5.
(2) Read, J. *J. Electrochem. Soc.* **2002**, *149*, A1190–A1195.
(3) Read, J.; Mutolo, K.; Ervin, M.; Behl, W.; Wolfenstine, J.; Driedger, A.; Foster, D. *J. Electrochem. Soc.* **2003**, *150*, A1351–A1356.
(4) Kuboki, T.; Okuyama, T.; Ohsaki, T.; Takami, N. *J. Power Sources* **2005**, *146*, 766–769.
(5) Ogasawara, T.; Débart, A.; Holzapfel, M.; Novák, P.; Bruce, P. G. *J. Am. Chem. Soc.* **2006**, *128*, 1390–1393.
(6) Read, J. *J. Electrochem. Soc.* **2006**, *153*, A96–A100.
(7) Kowalczk, I.; Read, J.; Salomon, M. *Pure Appl. Chem.* **2007**, *79*, 851–860.
(8) Mirzaeian, M.; Hall, P. J. *Power Syst. Technol.* **2007**, *31*, 90–96.
(9) Débart, A.; Bao, J.; Armstrong, G.; Bruce, P. G. *J. Power Sources* **2007**, *174*, 1177–1182.
(10) Débart, A.; Paterson, A. J.; Bao, J.; Bruce, P. G. *Angew. Chem., Int. Ed.* **2008**, *47*, 4521–4524.
(11) Girishkumar, G.; McCloskey, B.; Luntz, A. C.; Swanson, S.; Wilcke, W. *J. Phys. Chem. Lett.* **2010**, *1*, 2193–2203.
(12) Kraytsberg, A.; Ein-Eli, Y. *J. Power Sources* **2011**, *196*, 886–893.
(13) Padbury, R.; Zhang, X. *J. Power Sources* **2011**, *196*, 4436–4444.
(14) Freunberger, S. A.; Hardwick, L. J.; Peng, Z.; Giordani, V.; Chen, Y.; Maire, P.; Novák, P.; Tarascon, J.-M.; Bruce, P. Fundamental Mechanism of the Lithium-Air Battery. The 15th International Meeting on Lithium Batteries, Montréal, Canada, June 27−July 2, 2010; Abstract 830.
(15) Freunberger, S. A.; Chen, Y.; Peng, Z.; Griffin, J. M.; Hardwick, L. J.; Barde, F.; Novák, P.; Bruce, P. *J. Am. Chem. Soc.* **2011**, *133*, 8040–8047.
(16) Mizuno, F.; Nakanishi, S.; Kotani, Y.; Yokoishi, S.; Iba, H. *Electrochemistry (Tokyo, Jpn.)* **2010**, *78*, 403–405.
(17) Takechi, K.; Sudo, E.; Inaba, T.; Mizuno, F.; Nishikoori, H.; Shiga, T. Solvent Screening of the Electrolyte for Nonaqueous Li-Air Batteries. 218th ECS Meeting, Las Vegas, NV, October 10−15, 2010; Abstract 586.
(18) Mizuno, F. Fundamental Study on Rechargeable Reaction of Lithium-Oxygen Battery. Symposium on Energy Storage beyond Lithium Ion: Materials Perspectives, Oak Ridge, TN, October 7−8, 2010. https://www.ornl.gov/ccsd_registrations/battery/agenda.shtm.
(19) McCloskey, B. D.; Bethune, D. S.; Shelby, R. M.; Girishkumar, G.; Luntz, A. C. *J. Phys. Chem. Lett.* **2011**, *2*, 1161–1166.
(20) Xiao, J.; Hu, J.; Wang, D.; Hu, D.; Xu, W.; Graff, G. L.; Nie, Z. *J. Power Sources* **2011**, *196*, 5674–5678.

(21) Veith, G. M.; Dudney, N. J.; Howe, J.; Nanda, J. *J. Phys. Chem. C* **2011**, *115*, 14325–14333.
(22) Aurbach, D.; Daroux, M.; Faguy, P.; Yeager, E. *J. Electroanal. Chem.* **1991**, *297*, 225–244.
(23) Bryantsev, V. S.; Blanco, M. *J. Phys. Chem. Lett.* **2011**, *2*, 379–383.
(24) Peng, Z.; Freunberger, S. A.; Hardwick, L. J.; Chen, Y.; Giordani, V.; Bardé, F.; Novák, P.; Graham, D.; Tarascon, J.-M.; Bruce, P. G. *Angew. Chem., Int. Ed.* **2011**, *50*, 1–6.
(25) Laoire, C. O.; Mukerjee, S.; Abraham, K. M.; Plichta, E. J.; Hendrickson, M. A. *J. Phys. Chem. C* **2009**, *113*, 20127–20134.
(26) Laoire, C. O.; Mukerjee, S.; Abraham, K. M.; Plichta, E. J.; Hendrickson, M. A. *J. Phys. Chem. C* **2010**, *114*, 9178–9186.
(27) Frimer, A. A.; Rosenthal, I. *Photochem. Photobiol.* **1978**, *28*, 711–719.
(28) Sawyer, D. T.; Valentine, J. S. *Acc. Chem. Res.* **1981**, *14*, 393–400.
(29) Poupko, R.; Rosenthal, I. *J. Phys. Chem.* **1973**, *77*, 1722–1724.
(30) Frimer, A. A.; Farkash-Solomon, T.; Aljadeff, G. *J. Org. Chem.* **1986**, *51*, 2093–2098.
(31) Andrieux, C. P.; Hapiot, P.; Savéant, J.-M. *J. Am. Chem. Soc.* **1987**, *109*, 3768–3775.
(32) Frimer, A. A.; Gilinsky-Sharon, P.; Aljadeff, G.; Gottlieb, H. E.; Hameiri-Buch, J.; Marks, V.; Philosof, R.; Rosental, Z. *J. Org. Chem.* **1989**, *54*, 4853–4866.
(33) Collins, C. M.; Sotiriou-Leventis, C.; Canalas, M. T.; Leventis, N. *Electrochim. Acta* **2000**, *45*, 2049–2059.
(34) San Filippo, J., Jr.; Romano, L. J.; Chern, C.-I. *J. Org. Chem.* **1976**, *41*, 586–588.
(35) Gibian, M. J.; Sawyer, D. T.; Ungermann, T.; Tangpoonpholvivat, R.; Morrison, M. M. *J. Am. Chem. Soc.* **1979**, *101*, 640–644.
(36) Webster, R. D.; Bond, A. M. *J. Chem. Soc., Perkin Trans. 2* **1997**, 1075–1079.
(37) McDonald, R. N.; Chowdhury, A. K. *J. Am. Chem. Soc.* **1985**, *107*, 4123–4128.
(38) Stemmler, E. A.; Diener, J. L.; Swift, J. A. *J. Am. Soc. Mass Spectrom.* **1994**, *5*, 990–1000.
(39) Sawyer, D. T.; Chiericato, G., Jr.; Angells, C. T.; Nanni, E. J., Jr.; Tsuchiya, T. *Anal. Chem.* **1982**, *54*, 1720–1724.
(40) Katayama, Y.; Onodera, H.; Yamagata, M.; Miura, T. *J. Electrochem. Soc.* **2004**, *151*, A59–A63.
(41) Singh, P. S.; Evans, D. H. *J. Phys. Chem. B* **2006**, *110*, 637–644.
(42) Islam, M. M.; Ohsaka, T. *J. Phys. Chem. C* **2008**, *112*, 1269–1275.
(43) *Jaguar*, version 7.5; Schrödinger, LLC: New York, 2008.
(44) Straatsma, T. P.; Aprà, E.; Windus, T. L.; Bylaska, E. J.; de Jong, W.; Hirata, S.; Valiev, M.; Hackler, M.; Pollack, L.; Harrison, R.; et al. *NWChem, A Computational Chemistry Package for Parallel Computers*, version 5.1; Pacific Northwest National Laboratory: Richland, WA, 2007.
(45) Becke, A. D. *Phys. Rev. A* **1988**, *38*, 3098–3100.
(46) Lee, C. T.; Yang, W. T.; Parr, R. G. *Phys. Rev. B* **1988**, *37*, 785–789.
(47) Dunning, T. H., Jr. *J. Chem. Phys.* **1989**, *90*, 1007–1023.
(48) Kendall, R. A.; Dunning, T. H., Jr. *J. Chem. Phys.* **1992**, *96*, 6796–6806.
(49) Bryantsev, V. S.; Diallo, M. S.; William, A.; Goddard, W. A., III. *J. Phys. Chem. A* **2007**, *111*, 6796–6806.
(50) Møller, C.; Plesset, M. S. *Phys. Rev.* **1934**, *46*, 618–622.
(51) Purvis, G. D., III; Bartlett, R. J. *J. Chem. Phys.* **1982**, *76*, 1910–1918.
(52) Raghavachari, K.; Trucks, G. W.; Pople, J. A.; Head-Gordon, M. *Chem. Phys. Lett.* **1989**, *157*, 479–483.
(53) Watts, J. D.; Gauss, J.; Bartlett, R. J. *J. Chem. Phys.* **1993**, *98*, 8718–8733.
(54) Roberts, J. L., Jr.; Sawyer, D. T. *J. Am. Chem. Soc.* **1981**, *103*, 712–714.
(55) Chin, D. H.; Chiericato, G., Jr.; Nanni, E. J., Jr.; Sawyer, D. T. *J. Am. Chem. Soc.* **1982**, *104*, 1296–1299.
(56) Daasbjerg, K.; Lund, H. *Acta Chem. Scand.* **1993**, *47*, 597–604.
(57) Jensen, W. B. *Chem. Rev.* **1978**, *78*, 1–22.
(58) San Filippo, J., Jr.; Chern, C.-I.; Valentine, J. S. *J. Org. Chem.* **1975**, *40*, 1678–1680.
(59) Afanas'ev, I. B. *Superoxide Ion: Chemistry and Biological Implications*; CRC Press: Boca Raton, FL, 1990; Vol. 2.
(60) Pedersen, C. J. *J. Am. Chem. Soc.* **1967**, *89*, 7017–7036.
(61) Riess, G. R. *Chem. Rev.* **2001**, *101*, 2797–2920.
(62) Singh, S.; Verma, M.; Singh, K. N. *Synth. Commun.* **2004**, *34*, 4471–4475.
(63) Magno, F.; Bontempelii, G. *J. Electroanal. Chem.* **1976**, *68*, 337–344.
(64) Magno, F.; Bontempelii, G.; Andeuzzi Sedea, M. M. *J. Electroanal. Chem.* **1979**, *97*, 85–90.
(65) Bordwell, F. G.; Bartmess, J. E.; Hautala, J. A. *J. Org. Chem.* **1978**, *43*, 3095–3101.
(66) Bordwell, F. G.; Harrelson, J. A., Jr.; Lynch, T. Y. *J. Org. Chem.* **1990**, *55*, 3337–3341.
(67) McInture, R.; Scherson, D.; Storck, W.; Gerischer, H. *Electrochim. Acta* **1987**, *32*, 51–53.
(68) Yamaguchi, K.; Calderwood, T. S.; Sawyer, D. T. *Inorg. Chem.* **1986**, *25*, 1289–1290.
(69) Sawaki, Y.; Ogata, Y. *Bull. Chem. Soc. Jpn.* **1981**, *54*, 793–799.
(70) Baron, H.; Remfry, F. G. P.; Thorpe, J. F. *J. Chem. Soc., Trans.* **1904**, *85*, 1726–1761.
(71) Jeon, S.; Choi, Y. K. *Bull. Korean Chem. Soc.* **1995**, *16*, 1060–1064.
(72) Hassoun, J.; Croce, F.; Armand, M.; Scrosati, B. *Angew. Chem., Int. Ed.* **2011**, *50*, 2999–3002.
(73) Xu, K. *Chem. Rev.* **2004**, *104*, 4303–4417.
(74) Chamorro, E.; Perez, P. *J. Chem. Phys.* **2005**, *123*, 114107–10.